

# DIFFUSER ANGLE CONTROL TO AVOID FLOW SEPARATION

Vinod Chandavari<sup>1</sup>, Mr. Sanjeev Palekar<sup>2</sup>

M.Tech (APT), Department of Aerospace Propulsion Technology  
Visvesvaraya Technological University - CPGS  
Bangalore, Karnataka, India

<sup>1</sup>vinodchandavari@gmail.com, <sup>2</sup>aero.sanjeev@gmail.com

**Abstract**— Diffusers are extensively used in centrifugal compressors, axial flow compressors, ram jets, combustion chambers, inlet portions of jet engines and etc. A small change in pressure recovery can increase the efficiency significantly. Therefore diffusers are absolutely essential for good turbo machinery performance. The geometric limitations in aircraft applications where the diffusers need to be specially designed so as to achieve maximum pressure recovery and avoiding flow separation.

The study behind the investigation of flow separation in a planar diffuser by varying the diffuser taper angle for axisymmetric expansion. Numerical solution of 2D axisymmetric diffuser model is validated for skin friction coefficient and pressure coefficient along upper and bottom wall surfaces with the experimental results of planar diffuser predicted by Vance Dippold and Nicholas J. Georgiadis in NASA research center [2].

Further the diffuser taper angle is varied for other different angles and results show the effect of flow separation where it is reduced i.e., for what angle and at which angle it is just avoided.

**Keywords:** Planar Diffuser, CFD, Taper angle, Flow Separation.

## I. INTRODUCTION

Diffusers are integral parts of jet engines and many other devices that depend on fluid flow. Performance of a propulsion system as a whole is dependent on the efficiency of diffusers. Identification of separation within diffusers is important because separation increases drag and causes inflow distortion to engine fans and compressors. Diffuser flow computations are a particularly challenging task for Computation Fluid Dynamics (CFD) simulations due to adverse pressure gradients created by the decelerating flow, frequently resulting in separation.

These separations are highly dependent on local turbulence level, viscous wall effects, and diffuser pressure ratio, which are functions of the velocity gradients and the physical geometry. The diffuser is before the combustion chamber that ensures that combustion flame sustenance and velocities are small [2].

### 1.1 What is the meaning of Separation or Reverse Flow?

The designing of an efficient combustion system is easier if the velocity of the air entering the combustion chamber is as low as possible. The natural movement of the air in a diffusion process is to break away from the walls of the diverging passage, reverse its direction and flow back in the direction of the pressure gradient, as shown in figure 1.1 air deceleration causes loss by reducing the maximum pressure rise [4].

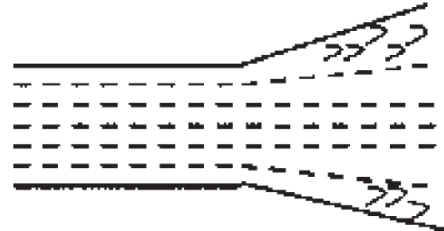


Fig: 1.1 Diffusing Flow

Buice, C.U. and Eaton, J.K [1], was carried out the experimental work using a larger aspect ratio experimental apparatus, paying extra attention to the treatment of the endwall boundary layers. They are titled as “Experimental Investigation of Flow through an Asymmetric Plane Diffuser.” The results of this experiment are compared to the results of different calculations made for the same diffuser geometry and Reynolds number. One of the calculations is Large Eddy Simulation (LES). The other is a Reynolds Averaged Navier Stokes (RANS) calculation using  $v^2$ -f turbulence model. Both calculations captured the major features of the flow including separation and reattachment.

Vance Dippold and Nicholas J. Georgiadis [2], they have been performed “Computational Study of Separating Flow in a Planar Subsonic Diffuser” in National Aeronautics and Space Administration is computed with the SST,  $k$ - $\epsilon$ , Spalart-Allmaras and Explicit Algebraic Reynolds Stress turbulence models are compared with experimentally measured velocity profiles and skin friction along the upper and lower walls.

Olle Tornblom [3], repeated the experimental work of Buice, C.U. and Eaton, J.K, “Experimental study of the turbulent flow in a plane asymmetric diffuser”, the flow case has been concentrated on in a uniquely composed wind-tunnel under overall controlled conditions. A similar study is made where the measured turbulence data are utilized to assess an explicit algebraic Reynolds stress turbulence model (EARSIM) and coefficient of pressure is measured.

In this study diffuser gives an idea of choosing the turbulence model and to avoid separation flow by varying the taper angle ( $7^\circ$ ,  $8^\circ$ ,  $9^\circ$  and  $10^\circ$ ).

The diffuser model and Fluent 14.5 are used, to study the diffuser characteristics with the effect of various factors like Pressure coefficient and Skin friction coefficient. Obtained results are validated against the known experimental results carried out by Vance Dippold and Nicholas J. Georgiadis [2].

## II. PHYSICAL MODEL AND MESH

Diffuser geometric configuration with the height of the inlet channel  $H = 0.015$  meters and the diffuser has a  $10^\circ$  expansion taper angle and is  $21H$  in length. At the end of the expansion, the diffuser channel is  $4.7H$  in height. Figure 2.1 shows the schematic diagram of diffuser [1].

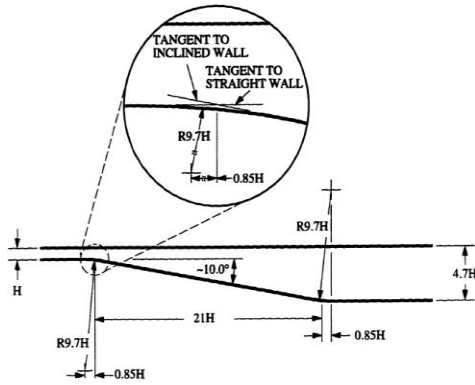


Fig: 2.1 Shows the schematic diagram of Diffuser

Figure 2.2 shows the computational domain of 2D that mimics the physical model. The diffuser apparatus can be divided into three sections: an inflow channel, the asymmetric diffuser, and an outflow channel. Figure 2.3 shows the 2D structured mesh for computational domain. Mesh having 41511 nodes and 41000 elements.

Mesh Quality:

Orthogonal Quality is ranges from 0 to 1, where values close to 0 correspond to low quality. Hence the

- Minimum Orthogonal Quality = 0.945334629648056
- Y plus value= 1.03

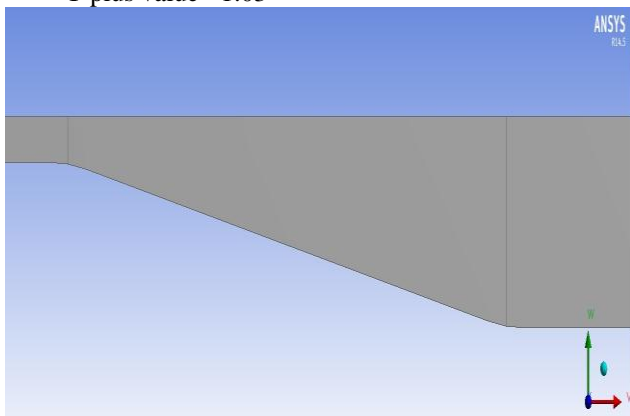


Fig: 2.2 Computational domain

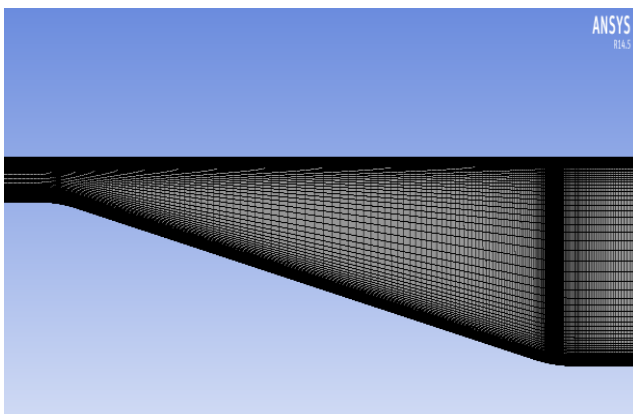


Fig: 2.3 Computational Domain with Mesh

### III. NUMERICAL PROCEDURE

This project implemented steady Reynolds Averaged Navier-Stokes equations (RANS) in the ANSYS FLUENT flow simulation program. For all cases, a two-dimensional, double-precision flow solver was used. It was assumed that the application of steady RANS equations was sufficient for this

Identical boundary conditions were used for all turbulence models. In particular, the inlet conditions were specified as a constant velocity profile corresponding to the bulk inlet velocity,  $U_b = 20$  m/s.

All turbulence models implemented a COUPLED scheme to couple the pressure and velocity. Furthermore, the spatial discretization was accomplished by a second-order accurate upwind scheme for the momentum and a FLUENT standard scheme for the pressure. Any additional closure equations for the various turbulence models were spatially discretized by second-order accurate upwind schemes. In all cases, the corresponding calculation residuals were monitored to convergence at  $1 \times 10^{-5}$ . These residuals included continuity, x-velocity, and y-velocity for all turbulence models. Beyond these generic residuals, any additional closure equations gave additional terms to monitor. The fluid properties were carefully chosen to ensure a matched Reynolds number with the experimental data. Specifically, the fluid density was chosen to be  $1.225$  kg/m<sup>3</sup> and the dynamic viscosity was selected to be  $1.789 \times 10^{-5}$  kg/m-s. The combination of these values yields the appropriate Reynolds number based on inlet channel height,  $Re_H = 20,000$ .

### IV. VALIDATION

The suitability of solver selection, turbulence model, numerical scheme, discretisation method and convergence criteria used in the present study is validated by comparing the skin friction coefficient and pressure coefficient along the X/H with the experimental data of Vance Dippold and Nicholas J. Georgiadis<sup>[2]</sup>. Among various turbulence models available in the fluent code, SST-k- $\omega$  model are tested with different taper angle (7°, 8°, 9° and 10°).

The figures 4.1.1 and 4.1.3 shows skin friction coefficient is 0.006 of Bottom\_wall and Top\_wall respectively, figure 4.2.1 shows the Pressure coefficient and the figure 4.1.2, 4.1.4 and 4.2.2 shows computational results obtained are in better agreement with the known experimental results as follows.

Table: 4.2 Comparison of Experimental Results with Computational Results

Parameters	Experimental	Computational				
		7°	8°	9°	10°	
Taper Angle	10°					
Pressure coefficient	0.73 to 0.85	0.882	0.880	0.873	0.85	
Skin friction coefficient	0.006 to 0.0063	0.0064	0.0065	0.0066	0.006	
Velocity (m/s)	Min	-1.156	0	-0.146	-0.723	-1.156
	Max	22.845	22.845	22.845	22.845	22.845

Table 4.2 demonstrates the correlation distinctive parameters of experimental results with computational results. This table demonstrates the how the taper angle decreases pressure coefficient expands and skin friction coefficient diminishes this implies the flow separation is bit by bit diminishes.

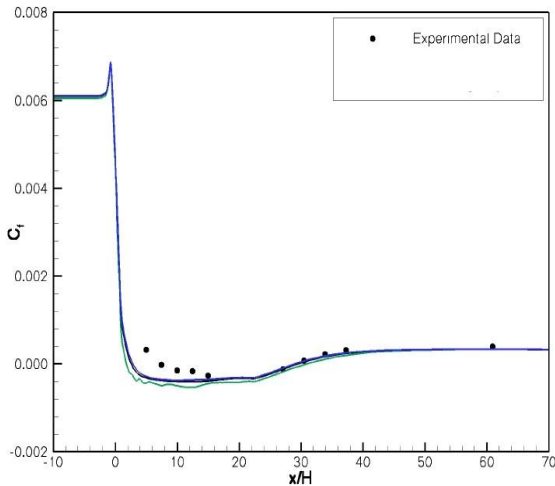


Fig. 4.1.1 Experimental results of Bottom\_wall skin friction along with the X/H using the SST model at 10° taper angle [2]

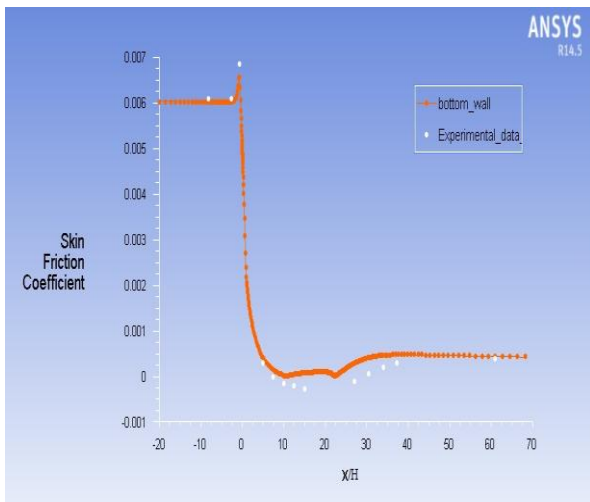


Fig. 4.1.2 Comparison of Computational Results with Experimental Results of Bottom\_wall skin friction along with the X/H using the SST model at 10° taper angle

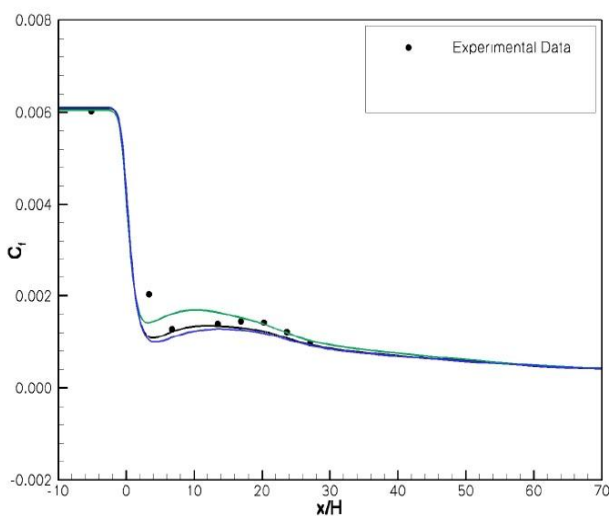


Fig. 4.1.3 Experimental results of Top\_wall skin friction along with the X/H using the SST model at 10° taper angle [2]

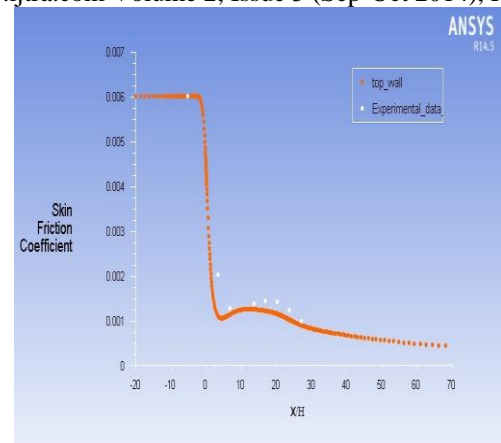


Fig. 4.1.4 Comparison of Computational Results with Experimental Results of Top\_wall skin friction along with the X/H using the SST model at 10° taper angle

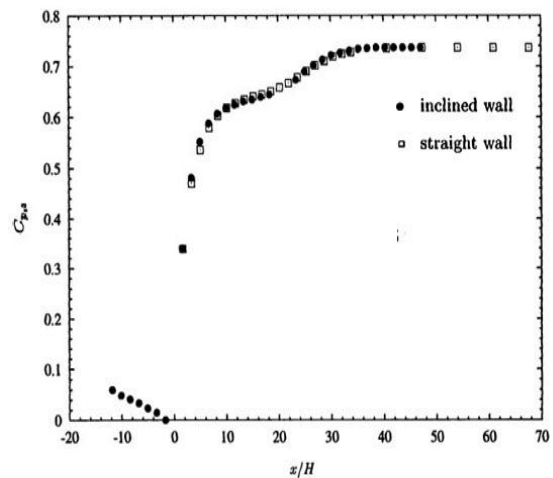


Fig. 4.2.1 Experimental results of pressure coefficient (Cp) at 10° taper angle along with the X/H

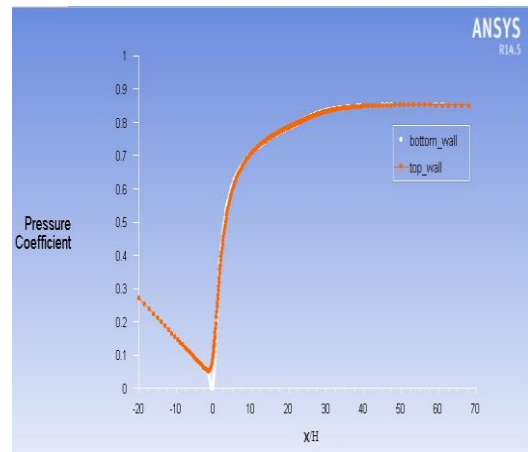


Fig. 4.2.2 Computational Results of Pressure Coefficient, bottom and Top wall at 10° taper angle

## V. RESULTS AND DISCUSSION

The results are obtained from the CFD by applying the experimental condition to the computational model with variation of taper angle 7°, 8°, 9°, and 10°, were measured for different contours plots, figure 5.1.1, 5.1.2, 5.1.3, and 5.1.4 shows the contours of velocity, figure 5.2.1, 5.2.2, 5.2.3, and 5.2.4 shows the separation for streamline functions and figure 5.2.5, 5.2.6, 5.2.7, and 5.2.8 shows contours of separation flow.

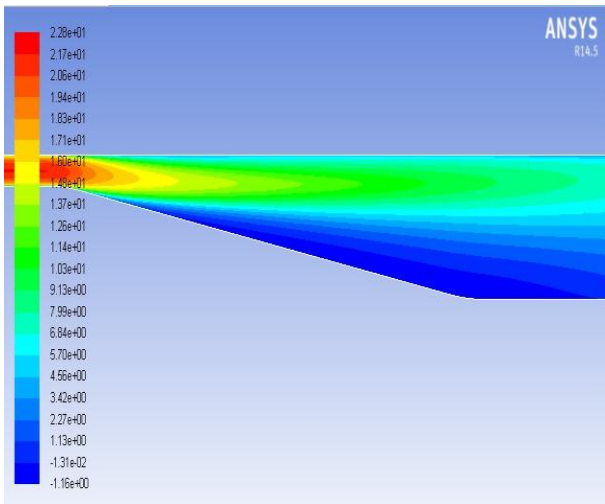


Fig: 5.1.1 Contours of Velocity at 10° taper angle

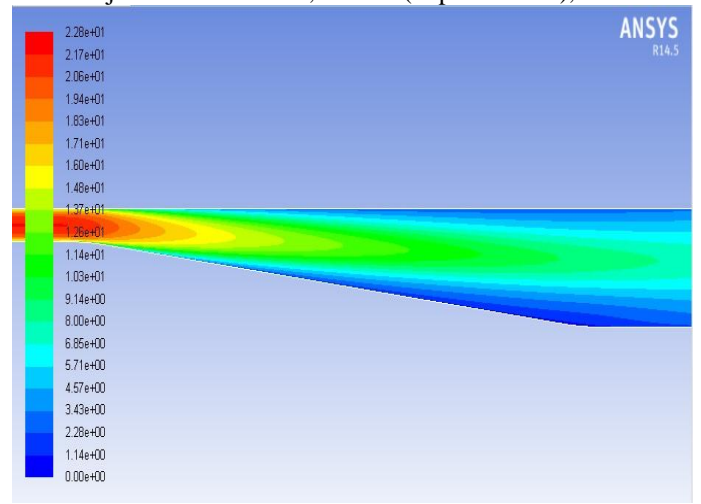


Fig: 5.1.4 Contours of Velocity at 7° taper angle

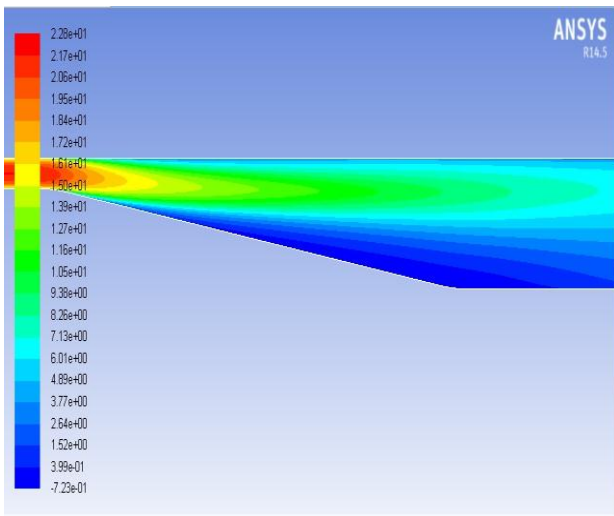


Fig: 5.1.2 Contours of Velocity at 9° taper angle

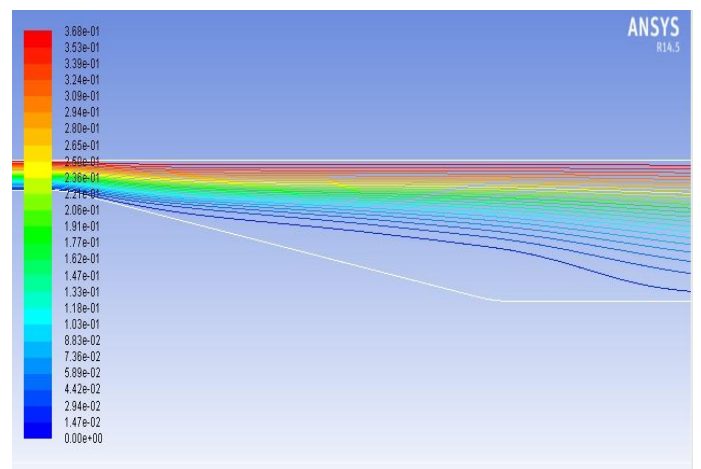


Fig: 5.2.1 Separation for Streamline Function at 10° taper angle

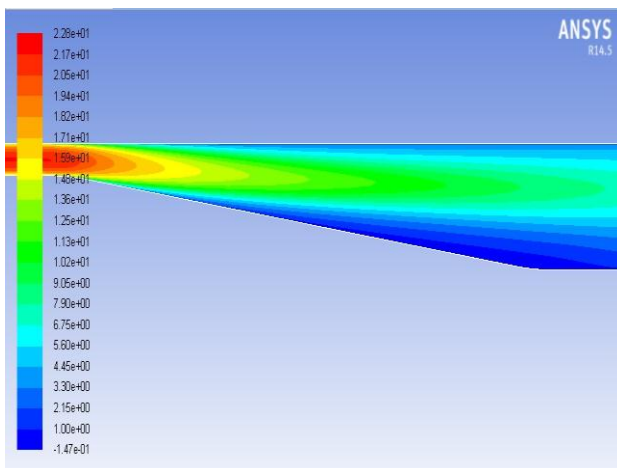


Fig: 5.1.3 Contours of Velocity at 8° taper angle

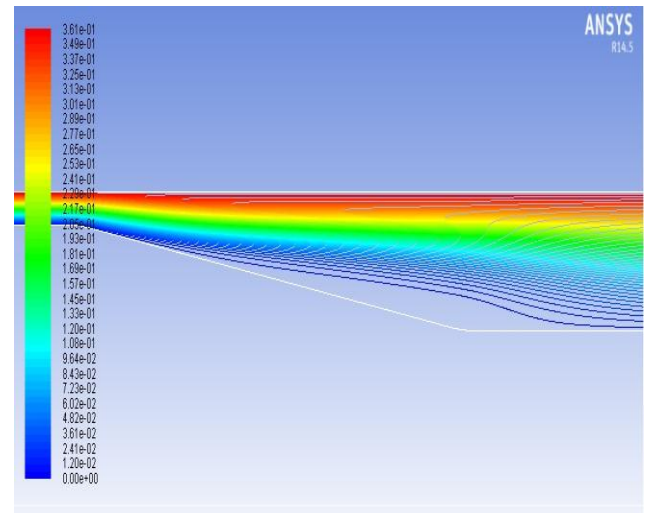


Fig: 5.2.2 Separation for Streamline Function at 9° taper angle

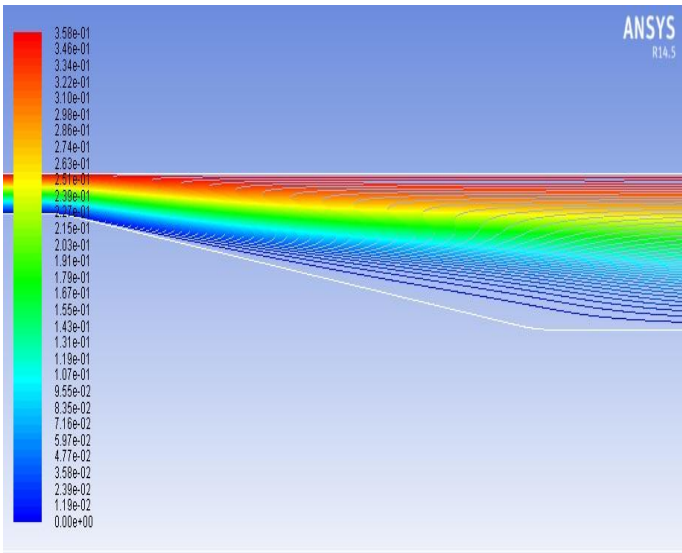


Fig: 5.2.3 Separation for Streamline Function at 8° taper angle

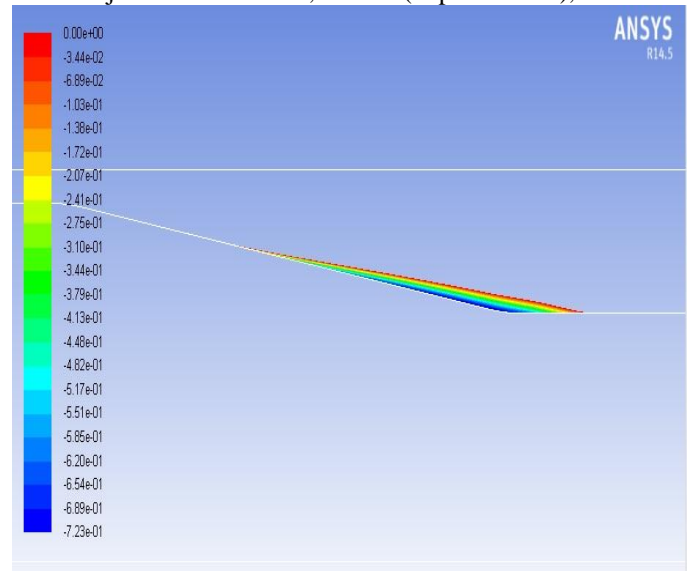


Fig: 5.2.6 Contours of Separation at 9° taper angle

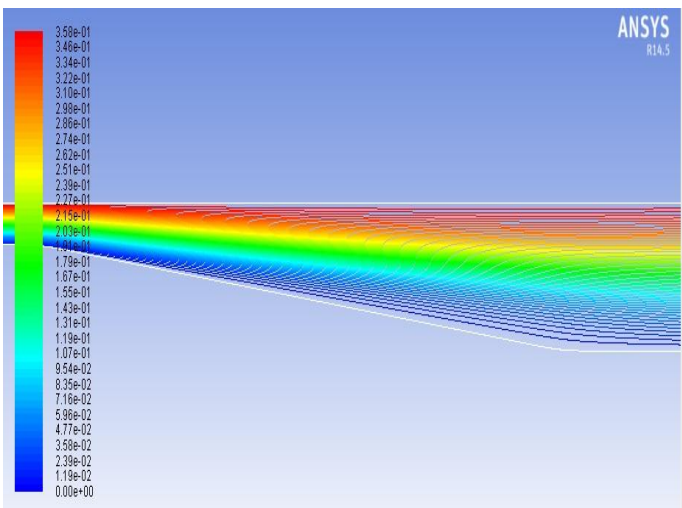


Fig: 5.2.4 Separation for Streamline Function at 7° taper angle

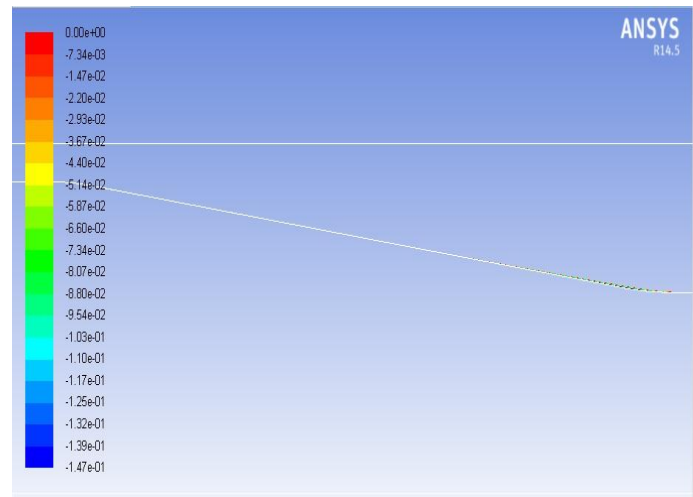


Fig: 5.2.7 Contours of Separation at 8° taper angle

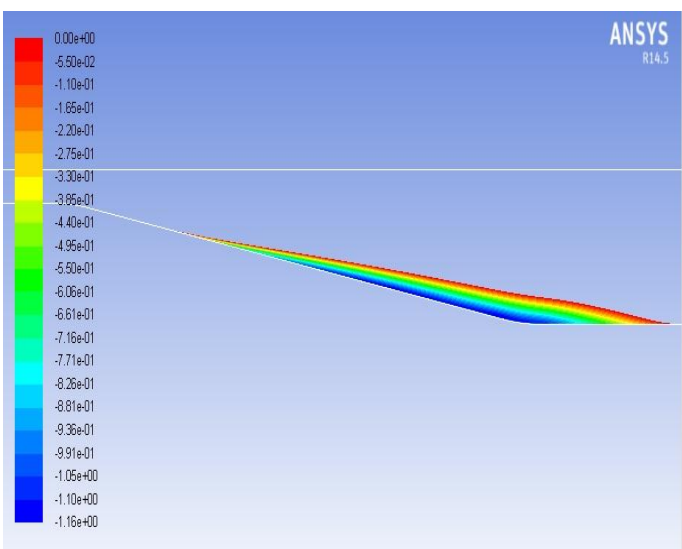


Fig: 5.2.5 Contours of Separation at 10° taper angle

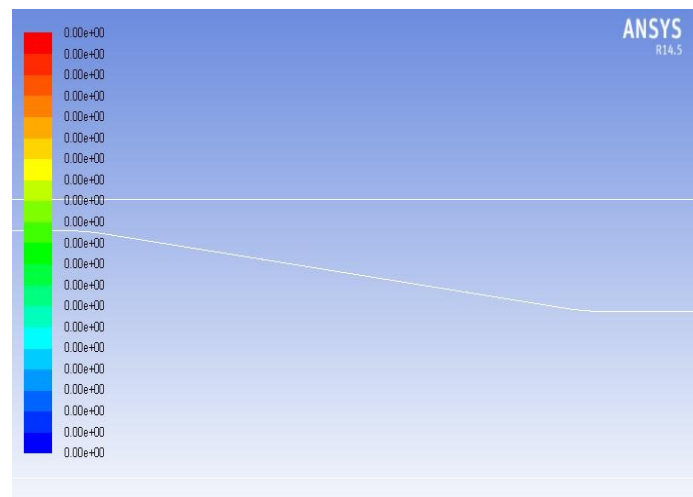


Fig: 5.2.8 Contours of Separation at 7° taper angle

Identification of separation within diffusers is important because separation increases drag and causes inflow distortion to engine fans and compressors.

Figure 5.1.1, 5.1.2 and 5.1.3 shows the contours of velocity 10°, 9° and 8° taper angle respectively, blue color shows the negative value. Figure 5.1.4 taper angle at 7° contours of

velocity doesn't shows negative value it means that the separation flow is avoided at  $7^{\circ}$  taper angle.

#### VI. CONCLUSION

From the present study it is evident that when the taper angle is decreased, the skin friction coefficient drops & pressure coefficient rises, as result the flow separation follows a diminishing trend

The optimum taper angle is  $7^{\circ}$  below which there is no flow separation at all but going beyond it gives rise to flow separation

#### VII. SCOPE FOR FUTURE WORK

The proposed next work for the present configuration is, simulating for 3D structured mesh configuration to these taper angle varieties and as in the present work the contrast in 2D taper angle we can figure it for variety taper angle, and 3D configuration simulation is possible for the impact of expectation taper angle.

#### REFERENCES

- [1] Buice, C.U. and Eaton, J.K., "Experimental Investigation of Flow Through an Asymmetric Plane Diffuser," 1997
- [2] Vance Dippold and Nicholas J. Georgiadis., "Computational Study of Separating Flow in a Planar Subsonic Diffuser," NASA, October 2005
- [3] Olle Tornblom., "Experimental study of the turbulent flow in a plane asymmetric diffuser," 2003
- [4] Reid A. Berdanier., "Turbulent flow through an asymmetric plane diffuser", Purdue University, April-2011
- [5] Arthur H Lefebvre and Dilip R. Ballal., "Gas Turbine Combustion-Alternative Fuels and Emissions", CRC Press Taylor & Francis Group, Third Edition pp.79 – 112 – 2010
- [6] Gianluca Iaccarino., "Predictions of a Turbulent Separated Flow Using Commercial CFD Codes," 2001
- [7] Obi, S., Aoki, K., and Masuda, S., "Experimental and Computational Study of Turbulent Separating Flow in an Asymmetric Plane Diffuser," Ninth Symposium on Turbulent Shear Flows, Kyoto, Japan, August-1993.
- [8] Dheeraj Sagar, Akshoy Ranjan Paul Et al., "Computational fluid dynamics investigation of turbulent separated flows in axisymmetric diffusers," 2011
- [9] E.M. Sparrow and J.P. Abraham., Et al. "Flow separation in a diverging conical duct: Effect of Reynolds number and Divergence angle," 2009.